
**STRUCTURE, PHASE TRANSFORMATIONS,
AND DIFFUSION**

Micro- and Nanoporous Structure Formed on the Titanium Surface by Laser Treatment

**I. G. Zhevtun^{a,*}, P. S. Gordienko^a, S. B. Yarusova^a, Yu. N. Kul'chin^b, E. P. Subbotin^b,
D. S. Pivovarov^b, and D. S. Yatsko^b**

^a*Institute of Chemistry, Far East Branch, Russian Academy of Sciences,
Vladivostok, 690022 Russia*

^b*Institute of Automation and Control Processes, Far East Branch, Russian Academy of Sciences,
Vladivostok, 690041 Russia*

**e-mail: jevtun_ivan@mail.ru*

Received May 30, 2017; in final form, August 24, 2017

Abstract—A microporous structure with controlled thickness of the porous layer and pore sizes has been prepared on the surface of VT1 titanium alloy by laser surface alloying of TiC powders and subsequent selective etching. It has been shown that the use of relatively coarse titanium-carbide powder particles, 80–100 μm, and the increase in the laser-beam speed to 20 mm/s allow us to form the uniform nanoporous substructure on the internal surfaces of pores.

Keywords: titanium alloys, composites, titanium carbide, microporous structure, laser

DOI: 10.1134/S0031918X18030134

INTRODUCTION

Porous materials based on ceramic materials, metals, and their carbides are widely used in mechanical engineering, metallurgy, aircraft, chemical, and other industries as filtering elements, lining, heat-insulating and transpiration-cooling materials, gas separators, catalyst supports, and sensors [1–5]. The extended-surface materials are also used to grow marine cultures [6]. Medical implants are no less promising and require the application of porous materials. A porous structure is an important feature for a surgical implant since a porous structure increases the specific surface area and favors the deeper integration of osseous tissue, which ensures adhesion strength between the osseous structures and implant [7]. Due to the combination of biocompatibility and corrosion-resistant and mechanical properties, titanium and its alloys are the main structural materials used in manufacturing implants. The toxicity of some metals, such as Ni, Cr, Co, and V [8], makes their presence in implant compositions impossible and determines the application of pure titanium.

Among the wide variety of methods for preparing microporous titanium-based structure, powder techniques, such as vacuum diffusion sintering [9, 10], self-propagating high-temperature synthesis (SHS) [11, 12], and pulsed current sintering [13] are widely used due to their practiced procedures and standard equipment. Other approaches to manufacturing titanium microporous materials are available. According to the data of [14], a frame preliminarily formed from a 0.4-mm-thick molybdenum wire was impregnated

with the titanium melt in a vacuum. After cooling the prepared composite, the molybdenum frame was subjected to selective etching, which in the formation of a porous article. According to the data of [15], a porous structure of ternary Ti–13Zr–13Nb titanium alloy was prepared by electrochemical reduction of preliminarily sintered titanium, zirconium, and niobium oxides with the CaCl₂ melt. The relatively high energy consumption of the above methods and high costs of equipment and starting components also determine the search for alternative approaches to forming microporous titanium-based materials.

According to the data of [16, 17], the micro- and nanoporous structure of titanium implants can be prepared by sandblasting their surfaces and subsequent acid etching. Titanium-based porous materials can be prepared using a mixture of fine-grained titanium alloy powders and various organic bindings [18]. An exciting and promising method that has received special attention in recent years consists in the layer-by-layer growth of porous article of a near-net shape using 3D printing and titanium powders. A powder can be melted using electron beam melting (EBM) [19, 20] and selective laser melting (SLM) [21].

Another approach to the formation of microporous structures on titanium alloys was suggested in [22], which consists in the plasma treatment of the surface to form a Ti–TiC-based composite and the subsequent selective etching of titanium carbide grains. An analogous approach was applied in [23] using both electric-arc treatment and laser irradiation. In the present paper, we report data on the formation of

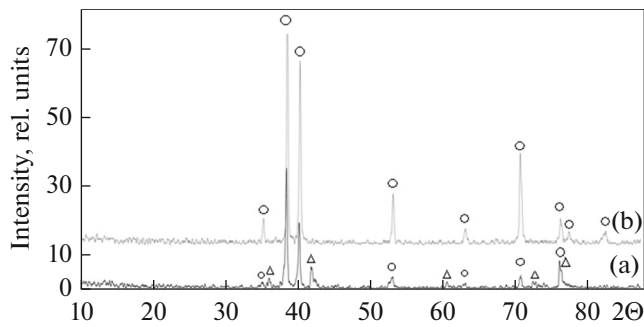


Fig. 1. X-ray diffraction patterns taken for the titanium alloy surface subjected to (a) laser treatment and (b) subsequent etching; symbols (○) and (△) correspond to Ti and TiC, respectively.

micro- and nanoporous titanium surface using laser treatment. Some peculiarities and advantages of the approach are noted.

EXPERIMENTAL

VT1-0 alloy samples $40 \times 40 \times 2$ mm in size were subjected to treatment by a laser beam moved along the surface; at the same time, a TiC powder was fed, and the melt was blown with argon. The TiC powder was fed coaxially by transporting-gas (argon) jet and was melted together with the substrate by a laser beam. We used two titanium carbide powders that differ in particle size, including titanium powders of less than $50 \mu\text{m}$ (TU 6-09-5050-82) and $80\text{--}100 \mu\text{m}$ (TU 3989-002-12606601-2006) in particles size. The laser surface alloying of powder is classified as an additive processes and, according to the ASTM F2792-12a standard, can be classified as directed laser deposition.

The sample surface was subjected to treatment using a universal robotized complex for the laser surface alloying of powders, which consists of a KUKAKR 30-3HA robot, a KUKA KRC4 control system, a KUKADKP-400 positioner, and the LC-1-K ytterbium fiber laser of $100\text{--}1000$ W in continuous laser-irradiation power (the wavelength is $\lambda = 1070 \mu\text{m}$). The following treatment parameters were used. The diameter of a laser beam at the treated surface is 0.6 mm, the laser-beam shift step between passes is 0.5 mm, and the distance between the nozzle surface and the treated object is 10 mm. The laser irradiation power P and laser-beam linear speed along the surface V_1 are variable parameters. During treatment, the used parameters are $P = 300, 400,$ and 500 W and $V_1 = 10$ and 20 m/s.

After treatment, sections of samples were prepared and subjected to selective etching using analytical-purity concentrated nitric acid. The surface was studied by scanning electron microscopy (SEM) using a Hitachi S5500 scanning electron microscope equipped with a Thermo Scientific energy-dispersive analyzer, a ZeisEVO 40XVP scanning electron micro-

scope equipped with an INCA 350 Energy analyzer, and an METAM LV41 optical inverter microscope. The average pore size and composite layer thickness h_c were estimated using graphical options of software available for the above instruments.

X-ray diffraction analysis was performed using a Bruker D8 ADVANCE diffractometer and $\text{CuK}\alpha$ radiation; X-ray diffraction patterns were processed using EVA software and the PDF-2 database.

RESULTS AND DISCUSSION

Figure 1 shows X-ray diffraction patterns for titanium samples subjected to surface laser treatment with titanium-carbide powder and subsequent selective etching. It is obvious that, in the course of laser treatment, titanium carbide particles enter into the titanium surface layer, and the Ti–TiC-based composite forms. This is indicated by reflections of both titanium and titanium carbide (Fig. 1a). Subsequent etching with nitric acid leads to the dissolution of TiC grains; in this case, only titanium is identified on the surface (Fig. 1b).

After the chemical etching of titanium carbide grains, the titanium surface is characterized by clearly observed porosity. It was noted in [23] that the thickness of the modified layer h_c can be controlled by varying the laser irradiation power and the speed of the laser beam. Figure 2 shows SEM images of the cross sections of surface layers prepared under different conditions using titanium carbide powder with a particle size of less than $50 \mu\text{m}$.

It follows from the electron micrographs that, when using fine-grained TiC powder with an average particle size of less than $50 \mu\text{m}$, the pore morphology and size remain unchanged under different treatment conditions, whereas the layer thickness varied in proportion to the irradiation power P and laser beam speed of $200\text{--}300$ (at $P = 400$ W and $V_1 = 20$ mm/s, Fig. 2a) to $350\text{--}600 \mu\text{m}$ ($P = 500$ W and $V_1 = 10$ mm/s, Fig. 2d).

By comparing the Ti–TiC-based composite layers prepared by electric arc [23] and laser techniques, it should be noted that, in the case of electrical arc technique, the layer thickness can reach $1\text{--}2$ mm and is difficult to control. Upon the selective etching of thick composite coatings, the penetration of the etching solution to the bottom of the layer is difficult due to the high dispersivity of titanium carbide grains. This can result in the presence of residual brittle titanium carbide phase under the porous layer formed after etching. This negatively affects the strength properties of the article. Therefore, to form a porous layer on the titanium surface that is free of residual carbides, the composite layer should be etched completely over its entire thickness; therefore, the composite layer should be relatively thin. Taking into account the maximum TiC grain size, which in the present study is $100 \mu\text{m}$, the layer thickness should be hundreds of microme-

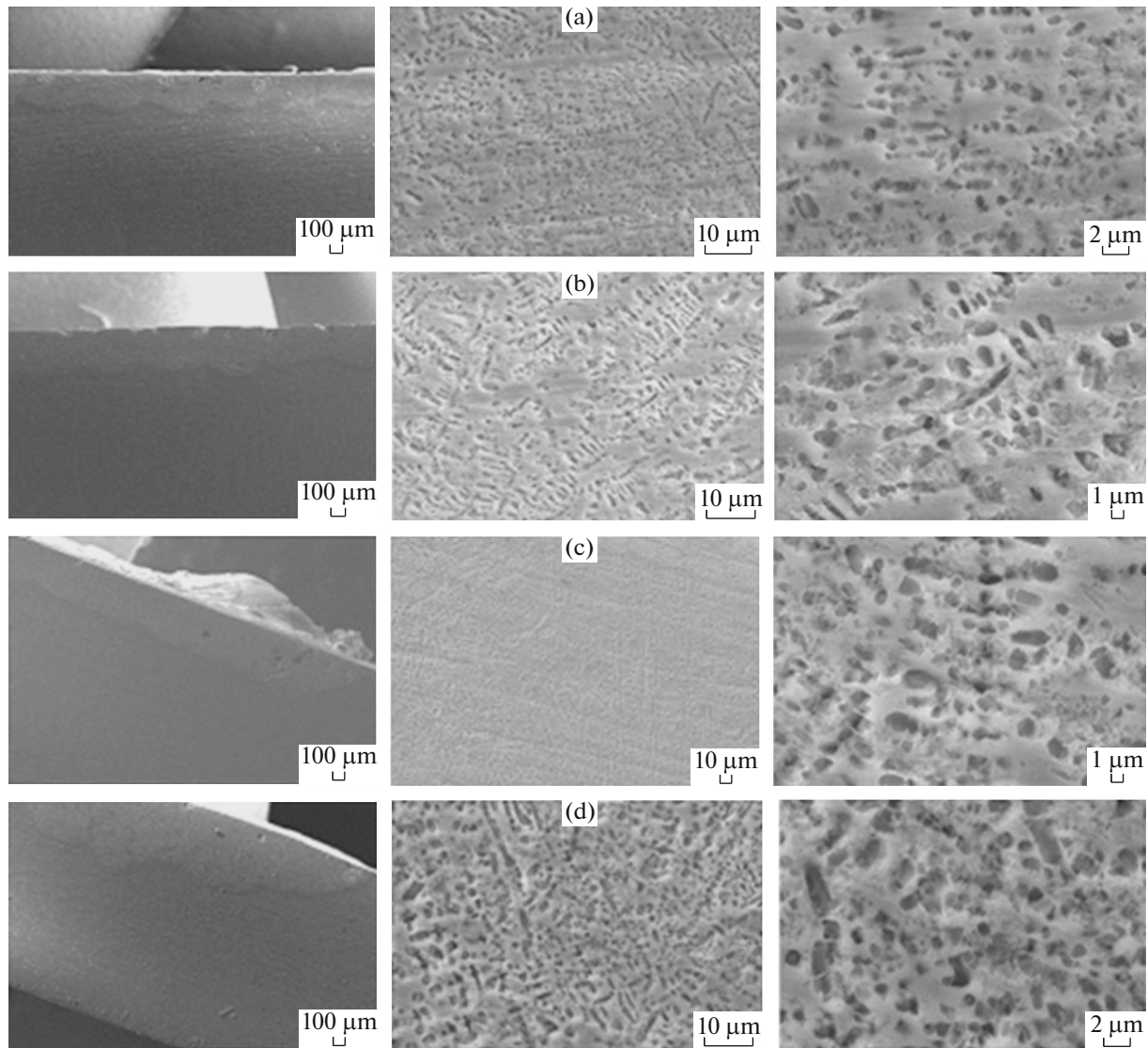


Fig. 2. Microstructure of surface layers formed on titanium under different conditions of laser treatment: (a) $P = 400$ W, $V_1 = 20$ mm/s, $h_c = 200\text{--}300$ μm ; (b) $P = 400$ W, $V_1 = 10$ mm/s, $h_c = 210\text{--}390$ μm ; (c) $P = 500$ W, $V_1 = 20$ mm/s, $h_c = 290\text{--}375$ μm ; and (d) $P = 500$ W, $V_1 = 10$ mm/s, $h_c = 350\text{--}600$ μm .

ters. The possibility of controlling the thickness of the modified layer favorably compares the laser surface treatment with the electrical arc treatment.

The possibility of controlling the pore sizes of porous coatings is another advantage of laser treatment used to form a porous coating. In the case of electric arc treatment, whatever the treatment conditions (a current range is 30–100 A), the characteristic size of the formed pores is 1–10 μm , whereas in the case of laser treatment, the pore size is determined by the used powder fraction (powder particle size). According to data given in Fig. 2, the pore size varies on average from 1 to 10 μm , although the length of individual dendrites, which are likely to result from the dissolution of titanium carbide grains in the titanium matrix, reaches 70–100 μm .

When a coarse TiC powder with an average particle size of 80–100 μm is used, a porous layer with the corresponding shape and pore sizes can be prepared (Fig. 3).

It should be noted that the pore distribution over the sample surface can also be controlled by varying the laser-treatment parameters, such as the volume of supplied powder, pressure of the carrier gas, and the distance between the nozzle plane and treated object.

In the course of the formation of porous layers that differ in the pore sizes on the titanium surface, it was found that, when the fine-grained powder of titanium carbide (with a particle size of less than 50 μm) is used, the sizes of pores formed after subsequent etching approximately correspond to the sizes of powder particles (Fig. 2). At the same time, when the relatively

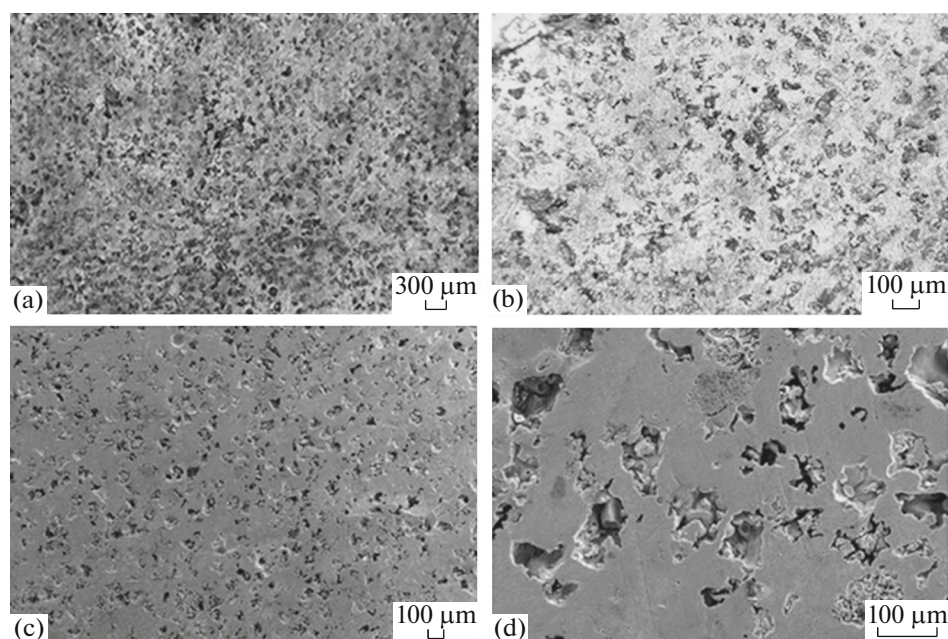


Fig. 3. (a, b) Optical and (c, d) SEM images of the surface of titanium samples subjected to laser treatment with TiC powder 80–100 μm in particle size and subsequent etching.

coarse TiC particles (80–100 μm) are used, along with pores that correspond in size to those of the particles, a uniform network of nanosized pores is formed on the internal surfaces of the pores that remain after the dissolution of the carbide grains. This two-level pore structure, i.e., nanosized pores formed on the internal surfaces of micropores, can be considered a nanoporous substructure. In this case, pores are formed between the basic large pores formed on the titanium sample surfaces, the sizes of which are smaller by 1–2 orders of magnitude than that of basic pores (Figs. 4a, 4c).

The average sizes of small pores on the outer sample surface and the internal surfaces of large pores range from 500 nm to 3–5 μm and 200–500 nm, respectively. According to the data of energy-dispersive analysis, the surfaces between and inside of pores (see Table 1) contain carbon, which likely indicates the partial dissolution of TiC in titanium, and free carbon present in the starting powder. Negligible contents of nitrogen and oxygen in the surface composition indicate the reaction between the surface melt and air despite that the treatment was performed in an inert atmosphere.

The formation of a porous substructure on the internal surfaces of large pores upon the laser treatment of a titanium surface is explained by the peculiar-

ities of the process of preparing the composite layer. In the course of treatment, TiC powder particles penetrate into titanium alloy surface molten by laser beam; in this case, due to the high temperature and surface-energy gradients, the active interaction of two phases takes place, which is accompanied by the redistribution of carbon between titanium and titanium carbides. Taking into account the fact that the melting and surface solidification processes are short-term ($\sim 10^{-3}$ – 10^{-4} s), which is typical of the laser treatment of metals, and a thin surface layer is fixed at the interface of two phases and forms a nanorough surface. Upon subsequent selective etching, the TiC phase is dissolved and a uniform network of nanosized pores forms at the carbide grain–melt interface.

It can be assumed that the above phenomenon is typical of laser treatment performed using relatively coarse carbide particles, since fine-grained TiC particles are characterized by substantially higher surface energy and, at the same temperatures, at the moment of the interaction of TiC with titanium melt, the redistribution of carbon between the carbide grain and the titanium matrix is more active.

In other words, the diffusion of carbon from coarse TiC grains into the titanium matrix is slower than in the case of fine grains and has no time to occur completely in the course of the short-term solidification of the melt. It was also noted that a pronounced nanoporous substructure is formed at a high laser-beam speed equal to 20 mm/s. As the speed decreases to 10 mm/s, the internal surface often becomes smooth (Fig. 5). This is likely to be related to the fact that, at a low laser-beam speed, more substantial surface heating leads to a decrease in the rate of melt solidification and favors the

Table 1. Element composition of titanium sample surface subjected to laser treatment using TiC powder with particle size of 80–100 μm and subsequent etching

Elements	Ti	C	N	O
Content (min–max), at %	80–100	0–10	0–5	0–5

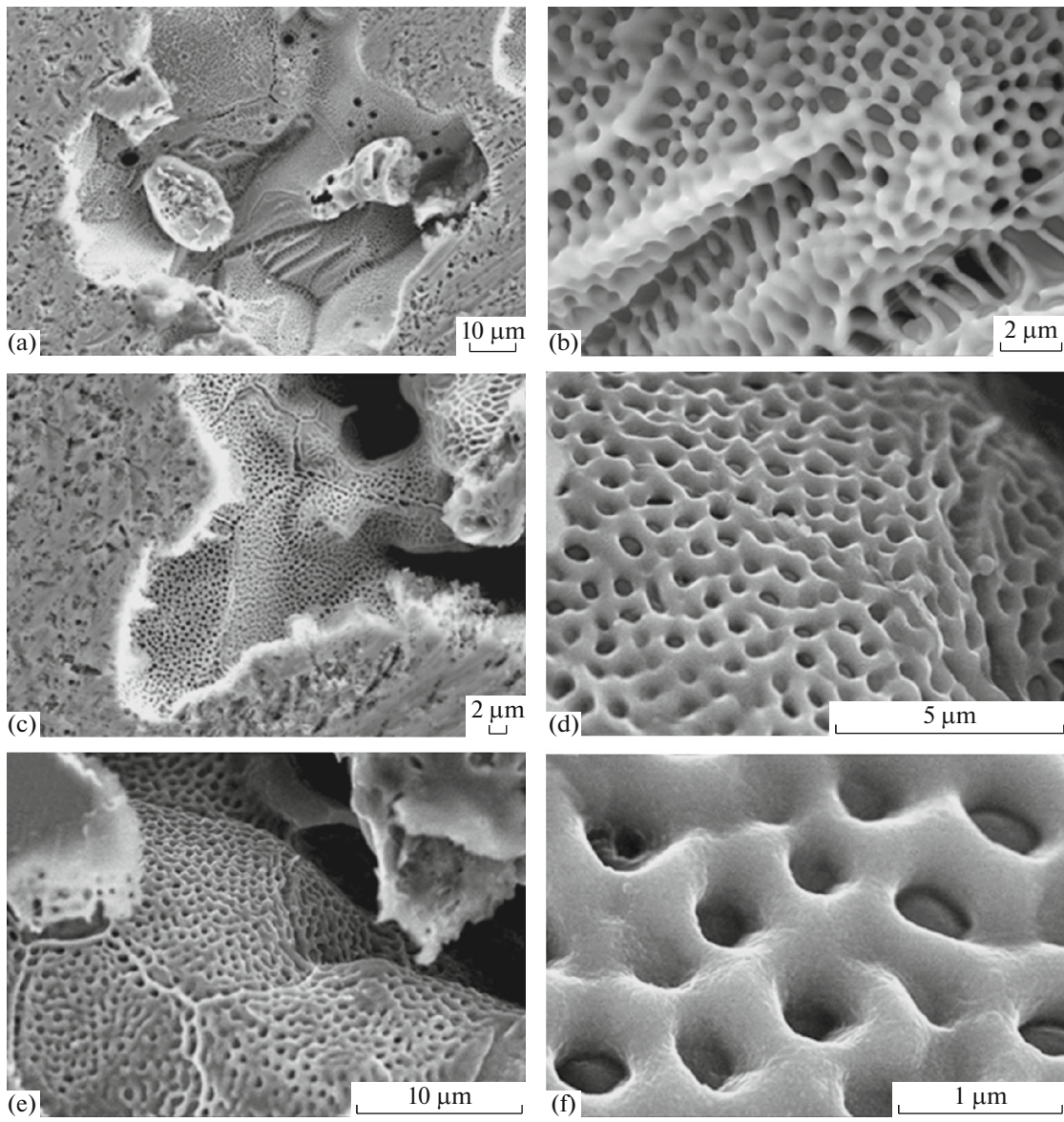


Fig. 4. Internal surface of pores formed on titanium surface subjected to laser treatment ($P = 300$ W and $V_l = 20$ mm/s) with TiC powder 80–100 μm in particle size and subsequent etching.

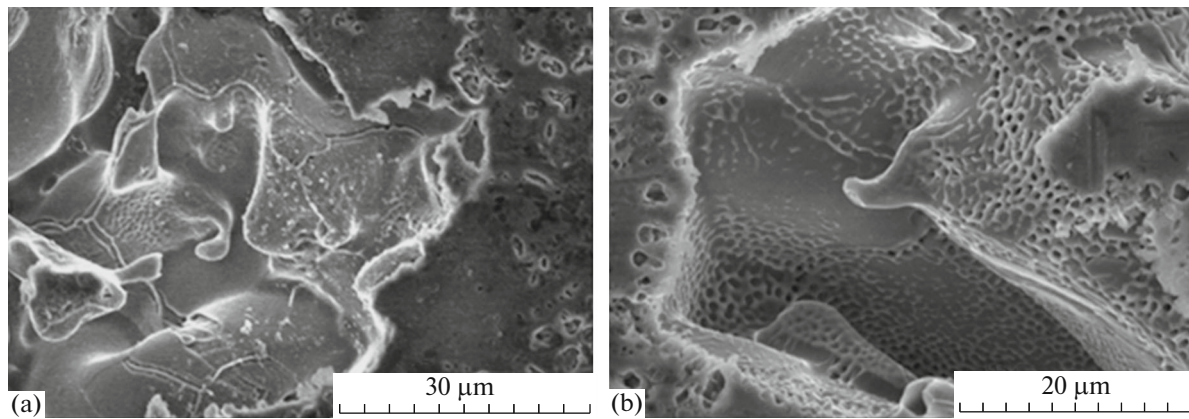


Fig. 5. Internal surface of pores formed on titanium surface subjected to laser treatment ($P = 300$ W and $V_l = 10$ mm/s) with TiC powder 80–100 μm in particle size and subsequent etching.

complete diffusion of carbon into the titanium matrix. As a result, the smoothing of the transition layer at the interface of two phases takes place.

The formation of a uniform porous substructure during the preparation of porous materials based on titanium and its alloys leads to a substantial increase in the total surface area. This in turn favors the firm adhesion of the impregnating material and matrix.

CONCLUSIONS

The porous surface of titanium can be obtained via the formation of the Ti–TiC–based composite layer upon alloying of refractory titanium-carbide particles on the titanium surface using laser irradiation and subsequent chemical etching of titanium carbide grains. The thickness of the porous layer and pore sizes can be controlled by varying the parameters of laser treatment, such as the irradiation power P , the speed of laser-beam motion V_1 along the treated surface, and the particle size of the powder. In view of this fact, the laser treatment favorably compares with the electrical arc method. A uniform nanoporous substructure is formed on the internal surfaces of pores using relatively large carbide powder particles of 80–100 μm , and $V_1 = 20$ mm/s.

ACKNOWLEDGMENTS

This study was supported by the Far East Branch, Russian Academy of Sciences (projects nos. 15-I-7-021 and 15-I-4-048).

REFERENCES

1. S. B. Belov, *Porous Materials in Machine Engineering* (Mashinostroenie, Moscow, 1976) [in Russian].
2. I. N. Sevost'yanova, V. Zh. Anisimov, S. F. Gnyusov, and S. N. Kul'kov, "Physicomechanical properties of porous titanium-carbide-based composites," *Fiz. Mezomekh.*, No. 7, part 2 (special issue), 89–92 (2004).
3. S. N. Kul'kov, S. F. Gnyusov, I. N. Sevost'yanova, and L. M. Molchunova, "Effect of the charge composition on the physicomechanical properties of porous permeable titanium-carbide-based materials," *Vopr. Materialoved.* **37** (1), 64–69 (2004).
4. M. I. Alymov, V. A. Zelenskii, and A. B. Ankudinov, "Porous material made of a titanium-carbide powder," *Perspekt. Mater.*, No. 4, 75–78 (2009).
5. L. Shi, H. Zhao, Y. Yan, Z. Li, and C. Tang, "Porous titanium carbide ceramics fabricated by coat-mix process," *Scr. Mater.* **55**, 763–765 (2006).
6. A. I. Railkin, *Colonization of Solid Bodies by Bottom Dwellers* (Izd-vo S.-Peterb. univ-ta, St. Petersburg, 2008) [in Russian].
7. V. V. Savich, D. I. Saroka, M. G. Kiselev, and M. V. Makarenko, *Modification of the Surface of Titanium Implants and Its Influence on Their Physicochemical and Biomechanical Parameters in Biological Media* (Belarus. navuka, Minsk, 2012) [in Russian].
8. M. Geetha, A. K. Singh, R. Asokamani, and A. K. Gogia, "Ti Based Biomaterials, the ultimate choice for orthopaedic implants—A Review," *Prog. Mater. Sci.* **54**, 397–425 (2009).
9. V. V. Astanin, E. Z. Kayumova, V. V. Nikitin, and A. I. Farkhetdinov, "Application of hydrogenated titanium powders for obtaining porous coatings on surgical implants using vacuum sintering," *Russ. Zh. Biomekhan.* **19** (1), 116–122 (2015).
10. C. E. Wen, Y. Yamada, and P. D. Hodgson, "Fabrication of novel TiZr alloy foams for biomedical applications," *Mater. Sci. Eng., C* **26**, 1439–1444 (2006).
11. V. R. Khodorenko, S. G. Anikeev, and V. E. Gyunter, "Structural and strength properties of porous titanium-nickelide prepared by the methods of SHS and sintering," *Izv. Vyssh. Uchebn. Zaved.* **57** (6), 17–23 (2014).
12. A. P. Amosov, I. M. Bairikov, A. E. Shcherbovskikh, E. I. Latukhin, A. F. Fedotov, K. S. Smetanin, Patent RF 2459686, 2012 [in Russian].
13. F. Zhang, L. Wang, P. Li, S. Liu, P. Zhao, G. Dai, and S. He, "Preparation of nano to submicro-porous TiMo foams by spark plasma sintering," *Adv. Engin. Mater.* **19** (2), 1–10 (2016).
14. D. Wang, Q. Li, M. Xu, G. Jiang, Y. Zhang, and G. He, "A novel approach to fabrication of three-dimensional porous titanium with controllable structure," *Mater. Sci. Eng., C* **71**, 1046–1105 (2016).
15. T. Yu, H. Yin, Y. Zhou, Y. Wang, H. Zhu, and D. Wang, "Electrochemical preparation of porous Ti–13Zr–13Nb alloy and its corrosion behavior in Ringer's Solution," *Mater. Trans.* **58**, 326–330 (2017).
16. Z. Wang, Y. Chen, and Z. Lin, Patent CN 102921037, 2013.
17. F. He, J. Shen, and H. Wang, Patent CN 104027839, 2014.
18. K. Kapat, P. K. Srivas, and S. Dhara, "Coagulant assisted foaming — A method for cellular Ti6Al4V: Influence of microstructure on mechanical properties," *Mater. Sci. Eng., A* **689**, 63–71 (2017).
19. K. C. Nune, R. D. K. Misra, S. J. Li, Y. L. Hao, and R. Yang, "Cellular response of osteoblasts to low modulus Ti–24Nb–4Zr–8Sn alloy mesh structure," *J. Biomed. Mater. Res. A* **105**, 859–870 (2016).
20. Y. J. Liu, H. L. Wang, S. J. Li, S. G. Wang, W. J. Wang, W. T. Hou, Y. L. Hao, R. Yang, and L. C. Zhang, "Compressive and fatigue behavior of beta-type titanium porous structures fabricated by electron beam melting," *Acta Mater.* **126**, 58–66 (2017).
21. R. Hedayati, A. M. Leeflang, and A. A. Zadpoor, "Additively manufactured metallic pentamode metamaterials," *Appl. Phys. Lett.* **110**, 091905 (2017).
22. I. G. Zhevtun and P. S. Gordienko, "Preparation of a microporous structure in titanium alloys," in *Proc. IV Int. Conf. on Chemistry and Chemical Technology, September 14–18, 2015, Yerevan, 2015*, pp. 186–188 [in Russian].
23. I. G. Zhevtun, P. S. Gordienko, S. B. Yarusova, V. E. Silant'ev, and A. A. Yudakov, "Preparation of a microporous structure on titanium alloys by the plasma treatment of the surface," *Fizikkh. Poverkhn. Zashch. Mater.* **53** (1), 91–95 (2017).

Translated by N. Kolchugina